Egyptian Geophysical Society
EGS Journal, Vol. 11, No. 1, 27-39 (2013)

CONTRIBUTION OF THE GEOLOGIC SETTING TO THE OCCURRENCE OF GROUNDWATER IN WADI MORRA, SOUTH SINAI, EGYPT, USING GEOELECTRICAL TECHNIQUES

A.A. Al-Abaseiry and A.M. Al Temamy

Department of Geophysics, Desert Research Center, El Matarya, Cairo, Egypt.

مساهمة الوضع الجيولوجى فى تواجد المياه الجوفية بوادى مرة، جنوب سيناء - مصر، باستخدام التقنيات الجيوكهربية

الخلاصة: وادى مره يمثل منطقة منخفضة و استكشاف المياه الجوفية فى هذا المنخفض يعتبر عنصر حيوي حيث سوف يتم إنشاء مجتمع جديد فى هذه المنطقة بالإضافة الى موقعها الاستراتيجي فى منطقة مشهورة بالسياحة بالإضافة الى الحاجة الملحة للمياه الجوفية لأغراض التنمية المختلفة. لهذه الأغراض تم استخدام التقنيات الجيوكهربية بمنطقة الدراسة لمعرفة التكوينات الحاملة للمياه الجوفية و لتوضيح تأثير عناصر التراكيب الجيولوجية على تواجد المياه الجوفية. لتحقيق هذا الغرض تم قياس عدد ١٢ جسه جيوكهربية رأسية فى صورة ثلاث قطاعات جيوكهربية و ٣ قطاعات للجيوكهربية المقطعية بمنطقة الدراسة. نتائج تفسير الجسات الكهربية أدت إلى التعرف على ثلاث وحدات جيوكهربية (A, B and C) وهى تكافىء رواسب العصر الرباعى، الحجر الرملى لتكوين عربة التابع لعصر الكمبرى و صخور القاعدة لعصر ما قبل الكمبرى على الترتيب. من هذه الدراسة تم التعرف على ثلاث طبقات متصلات حاملة للمياه الجوفية تابعة للوحدة الثانية. هذه الطبقات تمثل خزان جوفى إمكانات المياه به جيدة توجد تحت ظروف مقيدة إلى نصف مقيدة.

للاستفادة من النتائج و جعلها فى صورة بسيطة لمتخذي القرار تم تشييد خريطة لأولويات الحفر بمنطقة الدراسة. بالرغم من أن أولويات الحفر قاصرة على أماكن معينة إلا أن منطقة الدراسة تتميز عامة بإمكانات مياه جوفية عالية حيث أن أقل سمك للطبقات الثلاث يصل إلى ٨٣ متر فيما عدا مكان واحد شاذ إمكاناته أقل لوجود طبقتين حاملتين للمياه الجوفية به (جسة ١١).

فى ضوء هذه الدراسة تم التعرف على ٧ فوالق طبيعية من القطاعات الجيوكهربية التى تم تشييدها و خريطة مستوى سطح صخور القاعدة. هذه الفوالق لها تأثير على تواجد و إمكانات المياه الجوفية بمنطقة الدراسة. الطبقة الجيوكهربية الثالثة لم يتم التعرف عليها عند جسه ١١ لأن صخور القاعدة ذات عمق ضحل فى هذا المكان. هذه الفوالق تكون تتابعات متعاقبة و متبادلة من الأماكن المنخفضة و المرتفعة و بالتالي تؤثر على سمك الطبقات الحاملة للمياه الجوفية.

تم إجراء ثلاث قطاعات جيوكهربية مقطعية ثنائية الأبعاد عند ثلاث أماكن متعاقبة للتأكد من الفوالق التركيبية الناتجة من تحليل الجسات الجيوكهربية ووجد من تحليل بيانات هذه القطاعات و جود توافق تام بينهما.

ABSTRACT: *Wadi morra represents a morphotectonic depression in which Exploration for the groundwater is a vital element. As this area is important for touristic and development projects. Geoelectrical techniques are conducted to detect the water-bearing formation and to delineate the effect of geologic setting on the groundwater occurrence. The interpretation results of 12 Vertical Electrical Soundings (VES) in the form of three geoelectrical cross sections lead to the detection of three main geoelectrical units (A, B and C) which equivalent to Quaternary deposits, Cambrian sand of Araba Formation and Pre-Cambrian basement rocks, respectively. Three connected water-bearing layers belongs to unit B were detected. Therefore these connected layers represent a good aquifer which exists under confined to semi confined condition. The variation of the lithology and thickness laterally and vertically along these layers has an impact on the groundwater occurrence in the investigated area.*

In order to augment the feasibility of the geophysical results and to make them more illustrative and useful for decision maker, priority map for the groundwater exploitation have been constructed. Although the priority is restricted to the certain sites, the study area has generally, high groundwater potential where the lowest compiled thickness of the three water-bearing layers attains 83 m.

Seven normal faults were also detected from the constructed geoelectrical cross sections and the level to the top of the basement map. These faults have an impact on the occurrence of the groundwater in the concerned area, where they form consecutive alternation of grabens and horests which affect on the thickness of the water-bearing layers.

The two-dimensional imaging profiles were carried out at three consecutive selected sites with the purpose of verifying the detected structural faults. The interpretation results of these profiles are compatible with that of VES stations.

Key words: *Morphotectonic, depression, Groundwater, Geoelectric, Water-bearing, Vertical Electrical Soundings (VES), Faults, Two-Dimensional Electrical Imaging (2-D)*

INTRODUCTION

Wadi Morra represents a depression trending NW-SE structurally sandy plain at the extreme of upstream of Wadi Al Ghaib which debouch in Wadi Dahab (Hassnein, 2007). Its surface is covered with washed and drift sands that underlain by the sandstone of Araba Formation. As this area represents a plain area, it attracts the intention of South Sinai governorate to install a new community for the Bedwin people besides its importance for tourism activity.

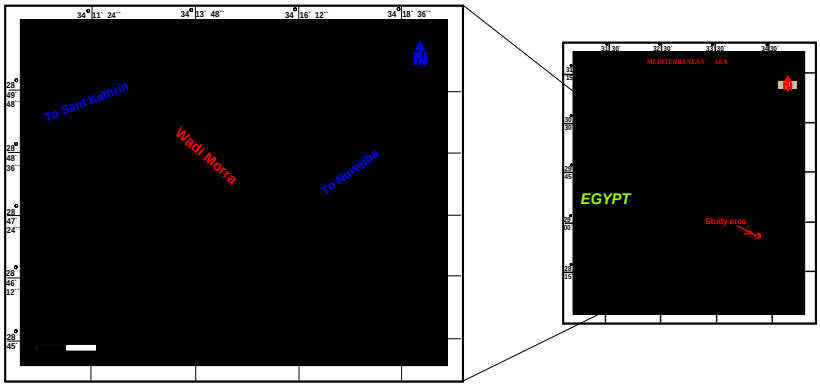

Fig. (1): The location map of the study area and the geoelectrical survey.

Therefore, the contribution of the geologic setting in exploring and occurrence of the groundwater along this district may represent the basis for different development objectives needed for both the tourism and the new community installation. Such contribution will be detected using geoelectrical techniques.

Wadi Morra is located in the south Sinai and follows the Gulf of Aqaba hydrographic province. It lies along the asphaltic road connecting between Nuweiba and Saint Katherine. It lies between latitudes 28° 45' and 28° 50.5' N, and longitudes 34° 12.5' and 34° 15.5' E (Fig.1) and covers an area of about 30 km ^{2}.

Climatic conditions:

The study area is located within the Mediterranean climatic condition zone. This zone is characterized by mild short winter with low erratic rainfall and hot long summer with high temperature and evaporation rates. The maximum air temperature attains 31°C in July at Saint Katherine (Hasanein, 2007). The mean annual rainfall is 38.2 mm at Saint Katherine. Heavy rainstorms occasionally occur with high intensity within few days in spring and autumn months. This in turn associated with torrential floods. The maximum relative humidity is recorded in December and January (45%, at Saint Katherine). The mean annual evaporation rate amounts to 3820 mm/year (Hasanein, 2007).

Geomorphologic elements:

The geomorphology of the concerned area and its vicinities has attracted the attention of many authors, among of them are Hammad and Misak (1985), Shabana (1999), Aggour (2000) and Hasanein (2007). The geomorphic units of Dahab basin illustrated by Hasanein (2007) include the watershed areas and the water collectors. The watershed areas comprise the mountainous terrain, El Tih southern scarp and the hilly terrain. On the other hand, the water collectors include inland morphotectonic depressions, Coastal plain and hydrographic basin. The investigated area includes the following geomorphic units:-

The relative air humidity is generally higher in winter than in summer. The maximum mean monthly value of evaporation is recorded in June (17.5 mm/day), whereas the minimum value, of about 5.6 mm/day, is recorded in January.

1- The mountainous terrain which covers the majority of Wadi Dahab catchments area is composed of acidic igneous and metamorphic rocks.

2- The hilly terrain exists at the northern part of Wadi Dahab basin. It is represented by residual sedimentary hills existed at the foot slopes of basement mountains. At Wadi El Ghaib, it is represented by faulted tilled block formed of sandstone, shale, marl and limestone.

3- The inland morphotectonic depressions which are oriented and owe their origin due to structural and erosion effects. Morra depression is an example of these depressions. It is a small NW-SE structural sandy plain (6 km long) and 3 km width) at the extreme of Wadi El Ghaib (tributary of Wadi Dahab). The slope of its surface is 13 m /km southeastward where its elevation varies between +920 m (NW) and +840 m (SE). It is covered by washed and drift sands that underlain by the sandstone of Araba Formation (G.S.E, 1994).

Geologic setting:

a- Lithology:

Lithologically, the area of study and its environs is covered by a wide varity of rock exposures. These exposures range from Precambrian basement rocks to the Quaternary alluvium deposits (Geologic Survey of Egypt, 1994). These are summarized as follows:

1-Pre-camprian:

The area of Wadi Dahab is mostly covered by fractured basement of late Proterozoic. These rocks consist of Dahab metadiorite, metavolcanic, quartz diorite and granodiorite, monzogranite and alkaline granite.

2- Cambrian:

Cambrian Araba Formation unconformably overlies the basement rocks (Hassan, 1967). Araba Formation measures 130 m thick at Wadi El Ghaib. It is composed of ferruginous varisized crossbedded sandstone with shale streaks. This formation is

unconformably underlies the Quaternary deposits at a depth of 66 m and extends up to 140 m in depth and its lower bottom didn't reach in the drilled well in the study area (Fig. 2, Regwa, 2009).

3-Quaternary:

Quaternary deposits cover the floor of the existing drainage network, the inland depressions and coastal plains. These deposits are composed of sandstone and gravels at the plains, while varisized gravel of igneous and metamorphic rock fragments embedded in the matrix of sand and clay dominate at the floor of channels. These deposits exhibit variable thickness which ranges from few meters to more than 40 m. in Dahab basin (Shabana, 1999). On the other hand, the Quaternary deposits consist of sand gravels and clay extends up to 66 m in the drilled well in the study area (Fig. 2).

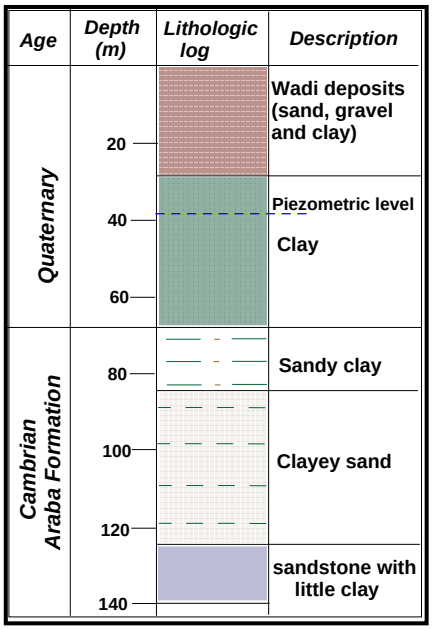

Fig. (2) Lithologic log of the drilled well (Regwa, 2009).

b- Structural setting:

South Sinai is situated in the northern part of the Arabian Nubian shield. The Arabian Nubian shield is a part of the East African Orogen formed in late Proterozoic (Bentor, 1985; Stern, 1994; Loizenbauer et al., 2001). Most structures in southern Sinai are related to accretionary events during closure of the Mozambique ocean and oriented roughly in NE to ENE (Shimron, 1984 and El Shafei et al., 1992).The NW and NE trends are nearly equals in abundance in the Precambrian and Cambrian whereas, the NW trends prevailed from Carboniferous to Holocene in Sinai Peninsula (Masoud and Koike, 2011).

The study area is located in East Sinai intensely faulted rift zone. Where, faulting is the major structural element. The existing faults constitute vast shear zone extends in NNE-SSW for 70 km length nearly parallel to the Gulf of Aqaba. The faults are mostly diagonal with great sinistral movement from few hundred meters to several kilometers (Eyal, 1981). This is evident from the displacement of the intersecting dykes and lithological contacts. This displacement is reduced to the west away from the Gulf.

Hydrogeologic setting:

The hydrogeologic setting of south Sinai was discussed by many authors. Some of them are Hassan (1967), Abdel Mogheeth et al. (1988), El Kiki et al. (1992), El Shamy (1992), El Ghazawi (1999), (Shabana (1999) and Hassanein (2007). The resources of groundwater in southern Sinai are variable. This is due to the pronounced differences in morphology of channel relief, nature depth to bed rock, thickness and texture of alluvium and the physical properties of the bounding cliffs as well as the local structure. The water-bearing formations in the south Sinai are represented generally by three main units; Quaternary alluvium, Nubian sandstone and Precambrian fractured basement (Hassanein , 2007).

In the study area, only one of these aquifer types was detected. This aquifer is the Araba Formation of Nubian sandstone aquifer. This aquifer was penetrated in one drilled well by Regwa company (2009) beside VES 7. The lithology of this aquifer ranges from sandy clay to clayey sand and ends with sandstone. This aquifer is present under confined condition. The water-bearing formation exists at depth ranges from 66m. to the end of the well (140 m.) whereas the depth to water in this aquifer is about 38 m. The peizometric level of this aquifer is + 815 m above sea level.

Geoelectrical studies:

Wadi morra represents a morphotectonic depression. Therefore, it is expected to have a large thickness of sedimentary cover which may have a good role in the occurrence of the groundwater. To achieve this target, geoelectrical techniques, in the form of Vertical Electrical Soundings (VES) and Two-Dimension Electrical Imaging are used in the following paragraph, a description of these field techniques is given:

a- Vertical electrical soundings:

A total of 12 Vertical Electrical Soundings (VES) were carried out in the investigated area (Fig. 3). Sounding station no.7 was conducted beside the drilled well (Fig. 2) to calibrate the VES values. Schlumberger configuration was applied with a distance between the two current electrodes starting from 2 meters and reaching 2000 meters.

A topographic survey was carried out to accurately locate the positions of the sounding stations, as well as the VES center point elevations.

b- Two-Dimensional (2-D) electrical imaging:

This geoelectrical technique was carried out along three profiles utilizing the Wenner array of electrodes. These Profiles were conducted around three consecutive

sounds (VESes 6, 7 and 8, respectively) to verify from the structural picture (consecutive alternation of horsts and grabbens) resulted from the constructed geoelectrical profiles of Vertical electrical Soundings interpretation data. So the three profiles have the same length (870 m) and the same unit of electrode separation (10 m.) which was increased at each traverse by unit multipliers to reach a maximum spacing of 290 m. (i.e. 10, 20, 30, 40 ....., 290 m). These profiles have NW-SE direction.

The Terrameter SAS 300 and Terrameter SAS 1000 resistivity meters were used during this survey for measuring the resistance "R" of each electrode separation.

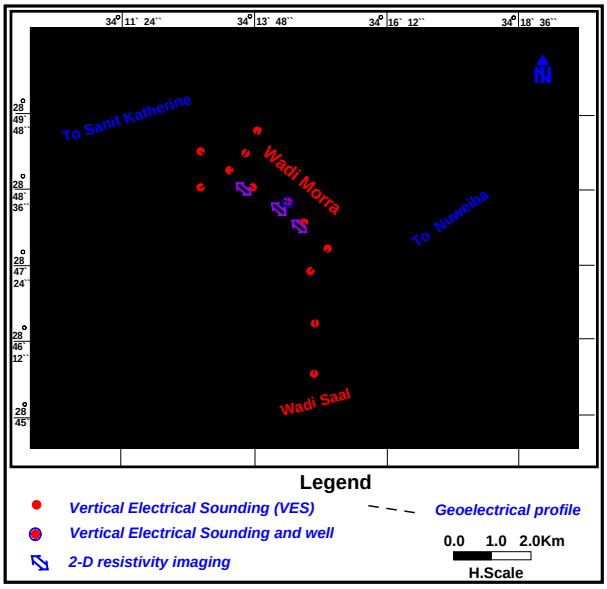

Fig. (3) Locations of the VES stations, geoelectrical profiles and two-dimension imaging profiles.

Interpretation of the Vertical Electrical Soundings Data:

The field data of the vertical electrical soundings have been interpreted qualitatively and quantitatively to delineate the subsurface sequence of the geoelectrical layers.

A-Qualitative interpretation:

Qualitative interpretation includes comparison of the relative changes in the apparent resistivities and thicknesses of the different layers. It gives information about the number of layers, their continuity, homogeneity, or heterogeneity of the individual layers.

Some of the VES curves in the study area is given in Fig. (4). The resistivity values of the first and second cycles of the resistivity curves are characterized by QQ, HKQ, and HK types (Telford et al., 1990) representing the surface and near surface conditions. This reflects the heterogeneity that characterizes the topmost layers. On almost the majority of the VES curves, the third cycle shows the same type (H-type) at different AB/2 distances, which reflects the homogeneity of lithology (high resistivity geoelectrical layer) of the deeper layer. At the same time, the last segment of the curve is present at different AB/2 distances (Fig. 4), which may reflect subsurface structural effects.

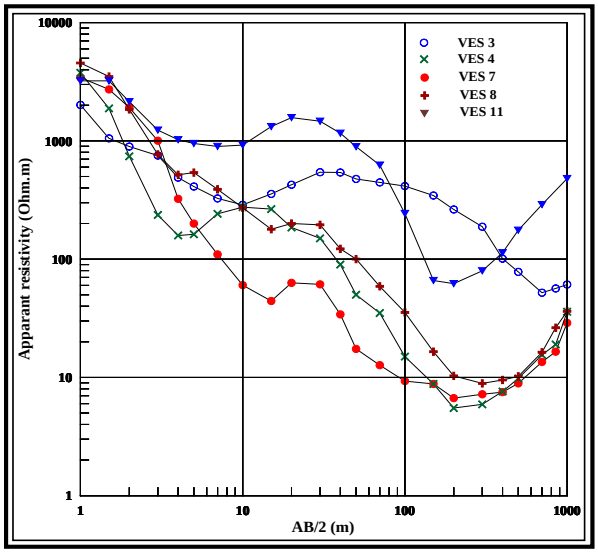

Fig. (4): Examples of the field VES curves of study area.

B-Quantitative interpretation:

For the quantitative interpretation of the geoelectrical resistivity sounding data, the computer programs "RESIST" (Velpen, 1988) and "RESIX-PLUS" (Interpex, 1996) have been used. They are interactive, graphically oriented, aid forward and inverse modeling programs for interpreting the resistivity curves in terms of a layered earth model. The lithologic data of the drilled well beside VES no. 7 and its corresponding hydrogeological data (Fig.3) are used to help in constructing the resistivity model, which is needed for adjusting the boundary of layers and calibrating the resistivity values of the water-bearing layers. The quantitative interpretation of the sounding measurements and the three constructed cross sections (A-A', B-B' and C-A' running in the NW-SE, NE-SW and N-S directions, respectively, Figs. 5, 6, and 7) in the area of study led to the detection of three main geoelectrical units (A, B and C), which correspond to Quaternary deposits, Cambrian Araba sandstone, and Precambrian basement rocks respectively. The ranges of resistivities and thicknesses of each unit are listed in table (1). A description of each of these units is given here after.

- **Unit A:**

This unit is differentiated into two geoelectric layers (A1 and A2) and their equivalent facies of dry Quaternary deposits.

a- The geoelectric layer "A1"consists of a group of thin layers. Its transverse resistivity values are ranging between 173 Ohm-m at VES 10 and 1758 Ohm-m at VES 11. The low resistivity corresponds to intruded clay with sand deposits of Quaternary alluvium, whereas the high resistivity value corresponds to boulders, gravel, sands and sandstone. The thickness of this layer varies from 15 m at VES 9 to 57 m at VES 1.

Table 1: Resistivities and thicknesses ranges, and their related lithologies.

Unit	Layer	Resistivity range (Ohm-m)	Thickness (m)	Lithology
"A"	A1	173 (VES 10) to 1758 (VES11)	15 (VES 9) to 57 (VES 1)	Gravel ,boulders, sands, clay and sandstone
	A2	1.2 (VES 7) to 18.6 (VES 2)	12 (VES1 1) to 4 6 (VES5)	Clay to sandy clay
"B"	B1	8 (VES 10) to 29 (VES 2)	16 (VES 9) to 26 (VES 5)	sandy clay to clayey sand
	B2	22 (VES 12) to 54 (VES 2)	13 (VES 1 1) to 56 (VES 3)	clayey sand to sand
	B3	75 (VES 8) to 125 (VES 2)	36 (VES 8) to 51 (VES 7)	Sandstone with some clay
"C"		1566 (VES 4) to 13740(VES11)	----------	Crystalline basement

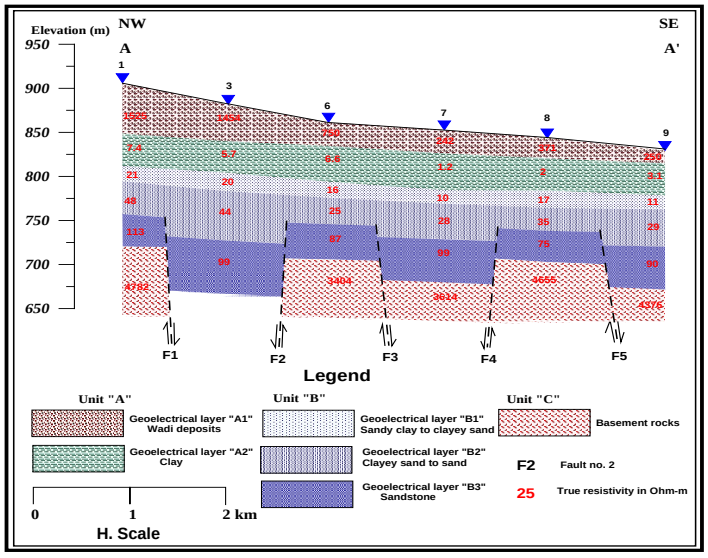

Fig. (5) Geoelectrical cross section A-A' along the main channel of Wadi Morra.

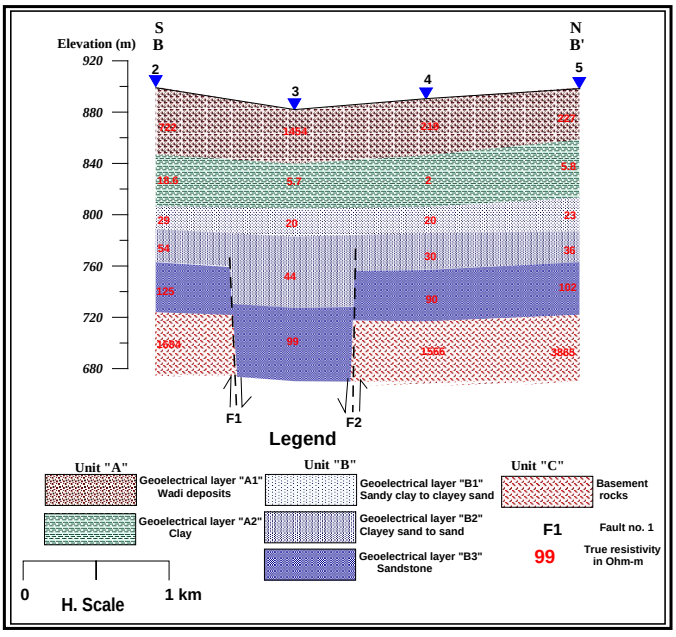

Fig. (6): Geoelectrical cross section B-B'.

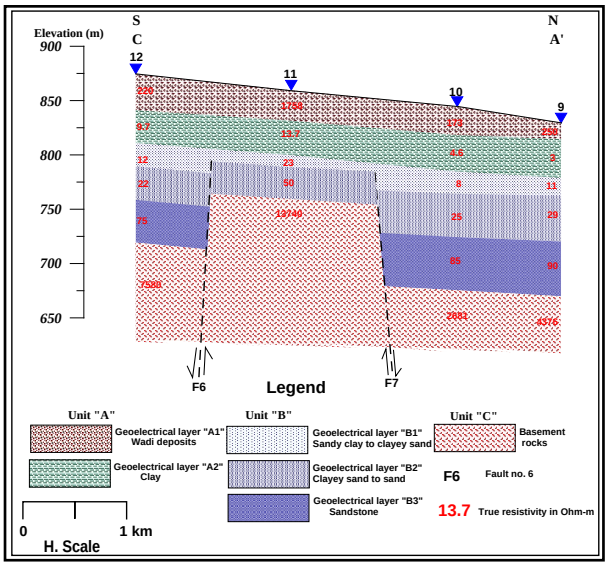

Fig. (7): Geoelectrial cross section C-A'.

b- The geoelectric layer "A2" has resistivity values varying from 1.2 Ohm-m at VES 7 to 18.6 Ohm-m at VES 2. The resistivity values of this layer correspond to clay to sandy clay deposits. The thickness of this geoelectric layer ranges between 12 m at VES 11 to 46 m at VES 5.

- **Unit B:**

This unit is differentiated into three geoelectric layers (B1, B2 and B3) and their equivalent facies of Cambrian Araba sands and clay facies. It represents the water-bearing formation in the study area.

a- The first geoelectrical layer "B1" lies below the clay to sandy clay of geoelectrical layer "A2". It has resistivity values ranging from 8 Ohm-m at VES 10 to 29 Ohm-m at VES 2 (Fig. 8A). This layer corresponds to sandy clay to clayey sand water-bearing. The thickness of this layer varies from 16 m. at VES 9 to 26 m. at VES 5 (Fig. 8 B).

b- The second geoelectrical layer "B2" has resistivity values ranging from 22 Ohm-m at VES 12 to 54 Ohm-m at VES 2 (Fig. 9A). This layer corresponds to clayey sand to sand water-bearing. The thickness of this layer varies from 24 m. at VES 5 to 56 m. at VES 3 (Fig. 9 B).

c- The last geoelectrical layer "**B3**" has resistivity values ranging from 75 Ohm-m at VES 8 to 125 Ohm-m at VES 2 (Fig. 10A). This layer corresponds to sandstone with some intruded clay water-bearing. The thickness of this layer varies from 36 m. at VES 8 to 51 m. at VES 7 (Fig. 10B).

- **Unit C**

The geoelectric unit "**C**" has resistivity values ranging from 1566 Ohm-m at VES 4 to 13740 Ohm-m at VES 11. This layer corresponds to crystalline basement. The depths to the basement surface in the study area range from 90 m at VES 11 to 186 m at VES 1.

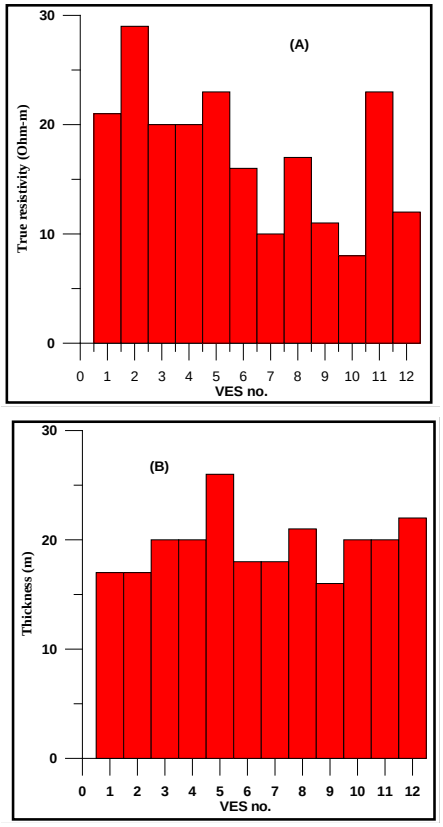

Fig. (8): Bar diagram of resistivity (A) and Thickness (B) distribution of layer "B1".

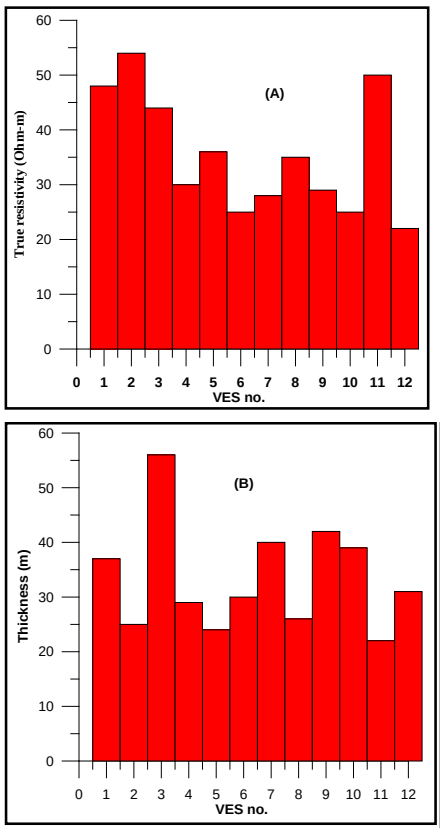

Fig. (9): Bar diagram of resistivity (A) and Thickness (B) distribution of layer "B2".

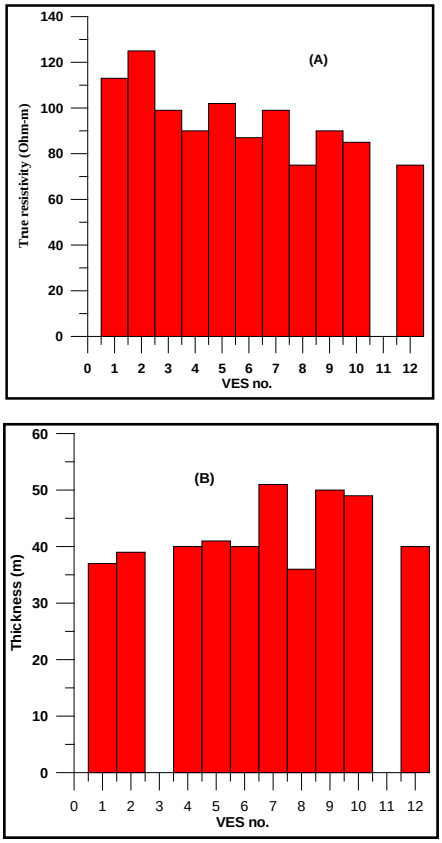

Fig. (10): Bar diagram of resistivity (A) and Thickness (B) distribution of layer "B3".

Based on the interpretation of the constructed geoelectrical cross sections, the following can be concluded:

1-Geoelectric layer "A1", A2, B1 and B2 were recorded at the all Vertical Electrical Soundings.

2-Geoelectric layer "B3" which represent the water-bearing sandstone was not detected at VES no. 11 (geoelectrical cross section C-A', Fig. 7).

3-The lower surface of geoelectric layer "B3" which represents sandstone water-bearing was not recorded at VES no. 3 with the used current electrode separation (AB/2 = 1000 m.)

4-The last detected geoelectric unit "unit C ", which represents the crystalline basement, was not detected with the used current electrode separation at VES no. 3 due to the structural effect.

Groundwater occurrences:

As mentioned above from the interpretation results of the Vertical Electrical Soundings, it could be concluded that, the water-bearing rock units in the area of study are represented by geoelectrical unit "B" which equivalent to Cambrian Araba Formation. This unit is differentiated into three geoelectrical layers (B1, B2 and B3) composed of sand, clay and sandstone with different ratios. The description of these layers will be discussed as follows:.

a- The first water–bearing layer (the geoelectric layer B1):

The results of the interpreted geoelectric data indicate that, the depths to the top of this layer generally decrease in the southeastern direction and increase in the northwestern trend (Fig. 11). It ranges from 52 m at the southeastern part (VES 9) to 94 m at the northwestern part (VES 1). Therefore, the groundwater flows regionally from the northwest to the southeast. This layer presents under confined to semi-confined conditions where the composition of the overlying layer (geoelectrical layer A2) ranges from clay to sandy clay deposits. The resistivity values of this aquifer (geoelectric layer B1) range between 8 Ohm-m at VES 10 and 29 Ohm-m at VES 2 (Fig. 8A) which corresponds to sandy clay to clayey sand deposits. The minimum saturated thickness of the concerned water-bearing layer is 16 m (VES 9), whereas the maximum recorded thickness is 26 m at VES 5 (Fig. 8B).

b- Second water–bearing layer (geoelectrical layer B2):

This layer represents a part of the Nubia sandstone (Cambrian Araba Formation).This geoelectrical layer is connected with the above water-bearing layer (B1) without confining. The groundwater flows regionally from northwest to the southeast.

The resistivity values of this aquifer (geoelectric layer B2) range between 22 Ohm-m at VES 12 and 54 Ohm-m at VES 2 (Fig. 9A) which corresponds to clayey sand to sand deposits. The minimum saturated thickness of this water-bearing layer is 24 m. (VES 5), whereas the maximum recorded thickness is 56 m. at VES 3 (Fig. 9B).

c- The third water–bearing layer (the geoelectric layer B3)

The depths to the top of this layer generally decrease in the southeastern direction and increase towards the northwest (Fig. 5). It ranges from 106 m at the southeastern part (VES 8) to 148 m at the northwestern part (VES 1). Therefore, the groundwater flows regionally from the northwest to the southeast. The resistivity values of this layer (geoelectric layer B3) range between 75 Ohm-m at VES 8 and 125 Ohm-m at VES 2 (Fig. 10A) which corresponds to sandstone water-bearing deposits. The minimum saturated thickness of the concerned water-bearing layer is 36 m. (VES 8), whereas the maximum recorded thickness is 51 m. at VES 7 (Fig. 10B). The bottom of this layer was not reached at VES 3 due to the structure effect. So, a larger thickness is expected at this site.

A priority map has been generated for exploiting Unit "B" (geelectrical layers B1, B2 and B3) in case of drilling deep wells. Since the resistivity and the thickness give indication about the quality and quantity of groundwater respectively, consequently each of them has been weighted by a factor of 40 %. As the depth to water is generally of shallow order therefore; the depth to this layer has been weighted by a factor of 20 %. For

the generation of the priority map, the transverse resistivity value for the three layers (ρT) estimated at each VES. Therefore, the thickness and depth to water has been categorized into four categories (table 2). The low resistivity values along this layer were given low category due to the high content of clay intruded with sand. On the other hand, the high resistivity values were given high category order where, the high values are expected to consist of saturated sand.

The groundwater priority map for the integrated three layers (B1, B2 &B3) in the investigated area (Fig. 12) indicates that, a local site at the northeastern part (VES 3) followed by the sites at the southeastern part (VES nos.9 followed by 10) represent the most promising sites for drilling well to exploit the groundwater.

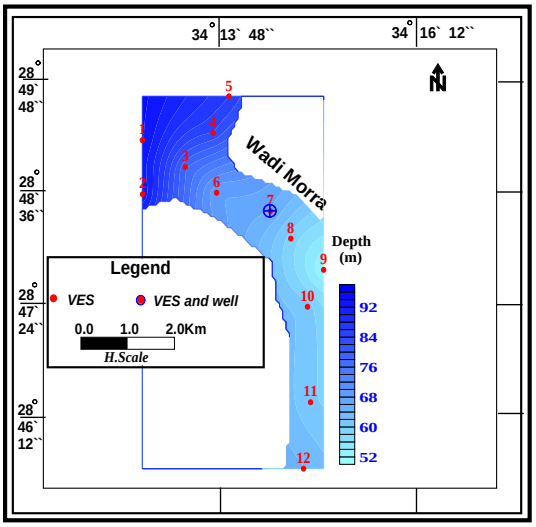

Fig. (11): Depth to water-bearing layer "B1".

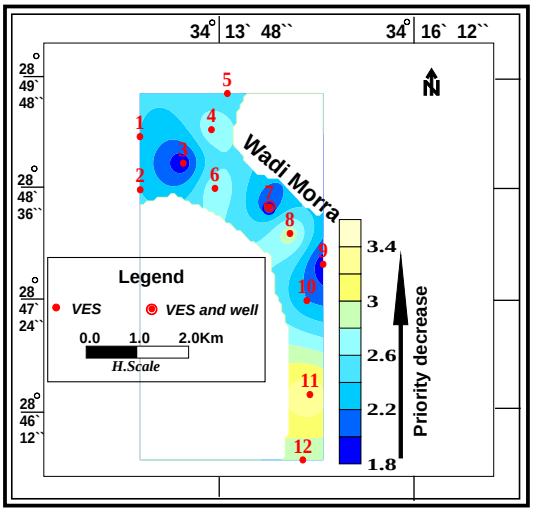

Fig. (12): Priority map for ground-water exploitation along geoelectrical layers "B1, B2 and B3".

In the light of this study, it can be concluded that, although the priority is restricted to certain sites, the study area has generally, high groundwater potential where the compiled thickness of the three water-bearing layers ranges between 83 m at VES 8 to more than 120 at VES 3. Anomalous low potential is restricted to the site of VES 11 where the third water-bearing layer was not detected.

The impact of geologic setting on the Ground water Occurrence:

The geologic setting impact comprises both the lithological variation and the structure impact on the water-bearing formation. The water-bearing formation in the study area is differentiated into three geoelectrical layers. These layers were found to vary vertically from sandy clay, clayey sand to sand in the first and second layers and finally to sandstone in the third layer. Therefore, the last geoelectrical layer is more beneficial for exploitation comparable with the first and second geoelectrical layers. On the other hand, each one of the three geoelectrical layers varies laterally. The first one (geoelectric layer B1) has resistivity values that range between 8 Ohm-m and 29 Ohm-m which corresponds to sandy clay to clayey sand deposits. The second geoelectrical layer (B2) has resistivity values, which vary from 22 Ohm-m to 54 Ohm-m which corresponds to clayey sand to sand deposits. The last geoelectrical layer (B3) has resistivity values that vary from 75 Ohm-m to 125 Ohm-m which corresponds to sandstone water-bearing deposits. Therefore, it could be concluded that, the sites have the highest resistivity values are preferable for the groundwater exploitation for both the first, second and third geoelectrical layers (B1, B2 and B3), where these sites are expected to have better groundwater quality.

Wadi Morra represents a morphotectonic depression, where the structure setting may play an important role in the occurrence of groundwater along the area of study.

To provide better insights into the structure setting impact on the groundwater occurrence in the investigated area, the Depth and level to the top of the basement surface were generated using the interpretation results of the VES measurements. As the bottom surface of the last water-bearing layer "B3" was not reached at VES 3, optimum value was given to this site to aid imagining the true position by constructing these maps. The constructed depth map to the basement surface (Fig. 13) revealed that, the depth to the basement surface is variable along the study area. The minimum depth value attaining 90 m. was recorded at the south (VES 11). On the other hand, the maximum value was recorded at the northwestern part (VES 3). Generally, the depth decreases from VES 3 to southeast wards except anomalous high and low value were detected at VES nos.7 and 8 respectively, due to expected structure effects. To be sure from this think, level basement map was constructed. The constructed level basement map (Fig. 14) revealed that, the level to basement surface is variable in the investigated area. It ranges from +650 m. at VES 3 to + 785 m. at VES 11. This map was used to deduce the structural elements

affecting the basement surface and in turn the thickness of the overlying water-bearing aquifer of Araba Formation (unit B). A group of normal faults (F1, F2, ……. and F7) have different trends were detected. These trends play an important role for the groundwater occurrence and potential in the study area. The faults F6 and F7 which have nearly E-W trends with downthrown side northward and southward, respectively, uplifted the basement rocks in this area (at VES 11). Therefore, Araba Formation deposits occur with a minor thickness (geoelectric layers B1 and B2) and the basement complex at this site contact on the other side of the fault a larger thickness of water-bearing Araba sand and sandstone (Geoelectrical layer B2 and B3 (Geoelectrical cross section C-A', Fig. 7). So this site has low groundwater potential.

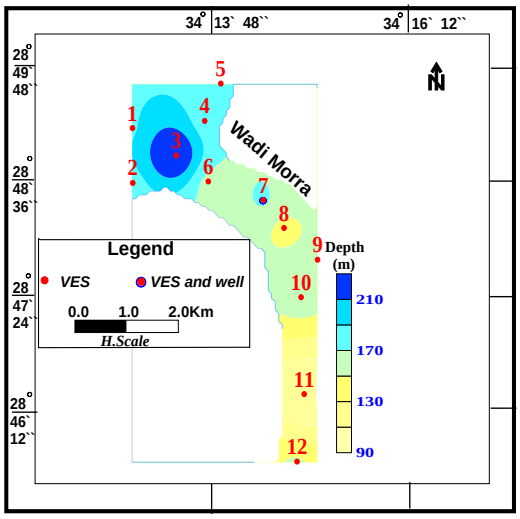

Fig. (13): Depth to basement contour map.

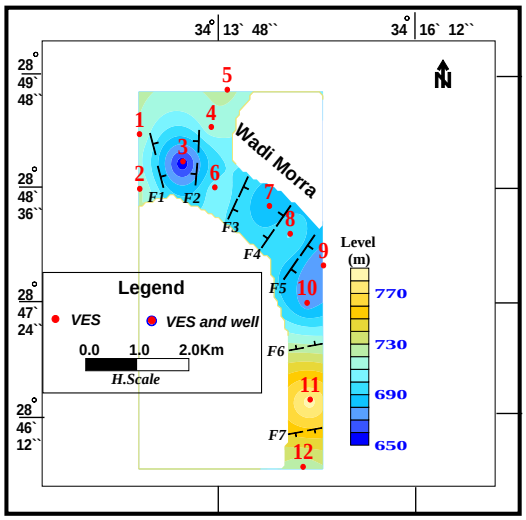

Fig. (14): Level basement contour map.

The faults from F1 to F6 form consecutive alternation of low and high basement surfaces along the NW-SE main channel of Wadi Morra. The faults F1 and F2 which have NNW and NNE trends with downthrown side east and west wards respectively, lead to the formation of a graben between the two faults. Therefore, The Araba sandstone (geoelectric layer B3) in this site contacts a basement complex on the other side of the fault. A similar concept is found between the faults F3 and F4 which trend NE with downthrown side east and west wards respectively, leading to the formation of a grabben between these two faults (at VES 7). The same last concept is detected between the faults F5 and F6 which trend NE and E-W with downthrown side SE and N wards respectively, leading to the formation of a graben between these faults (at VES nos. 9 and 10). On the other hand, two horsts between each of the faults F2 and F3 (at VES 6) and F4 and F5 (at VES 8) respectively, adjacent to the above discussed grabens. Therefore, Araba Formation deposits occur with a smaller thickness (geoelectric unit B) and the uplifted basement complex at these sites contact on the other side of the fault a larger thickness of water-bearing Araba sand and sandstone (Geoelectrical layer B3, geoelectrical cross section A-A', Fig.5).Therefore, it could be concluded that, the geologic setting has a decisive role on exploring, occurrence and potential of groundwater along the study area.

Interpretation results of the two-dimensional imaging data:

To augment the reliability of the VESes results and the deduced structures from the constructed geoelectrical cross-sections, the measured two-Dimension Imaging data at three sites in the study area was interpreted. A forward modeling subroutine was used to calculate the apparent resistivity values. A non-linear least-square optimization technique is used for the inversion routine (De Groot-Hedlin and Constable, 1990, and Loke and Barker, 1996a**).** The interpretation of the 2-D resistivity data has been carried out by using the computer program RES2DINV, ver. 3.4 written by Loke (1998). It is a Windows-based computer program that automatically determines a two-dimensional (2-D) subsurface resistivity model for the data obtained from electrical imaging surveys (Griffiths and Barker, 1993).

The true resistivity plot of the 2-D imaging profile at site one (Fig. 15) indicates that, this model consists of three zones, according to the resistivity values along the profile. The upper zone is mostly dry and consists of two layers which are equivalent to the Quaternary alluvium. The upper layer has a wide resistivity range that varies from about 285 to more than 1000 Ohm-m. This zone is equivalent to the dry gravel, boulders, sand and sandstone. The thickness of this layer reaches as much as 28 m. The second layer has a resistivity values ranging from 1 to 8 Ohm-m which corresponds to clay deposits. This layer extends to a depth of about 68 m. The second zone represents the water-bearing formation and its resistivity values increase with depth from about 17 Ohm-m to about 170 Ohm-m. Therefore, the clay content decreases with depth and inversely, sand and sandstone percentage increase. This layer has a small thickness in SE direction (62 m.) whereas its thickness increases in NW direction.

Table (2): Resistivity, thickness and depths to water category ranges for the integrated geoelectrical layers "B1, B2 and B3".

Category	Transverse Resistivity (ρT) ranges (Ohm-m)	Thickness (h) Ranges (m.)	Depth (D) ranges (m.)
1	ρ ≥ 72	h ≥ 108	52≤ D < 63
2	62≤ ρ < 72	86≤ h < 108	63≤ D < 73
3	52≤ ρ < 62	61≤ h < 86	73≤ D < 83
4	42≤ ρ < 52	36≤h < 61	D ≥ 83

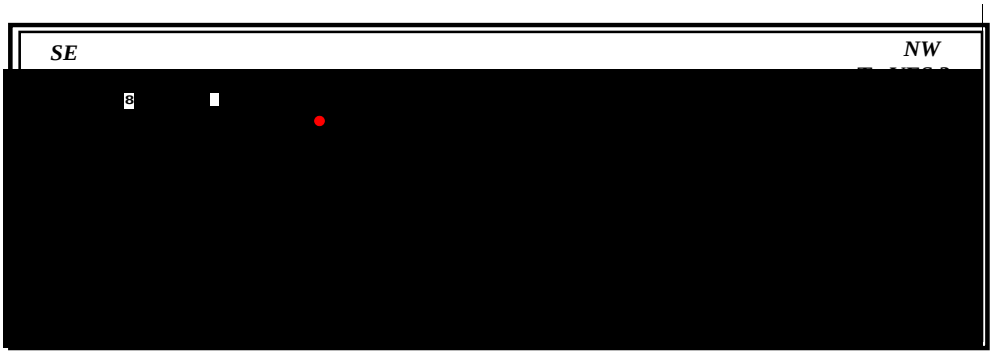

Fig. (15): Inverted resistivity model of the Two-Dimension imaging profile at the first site.

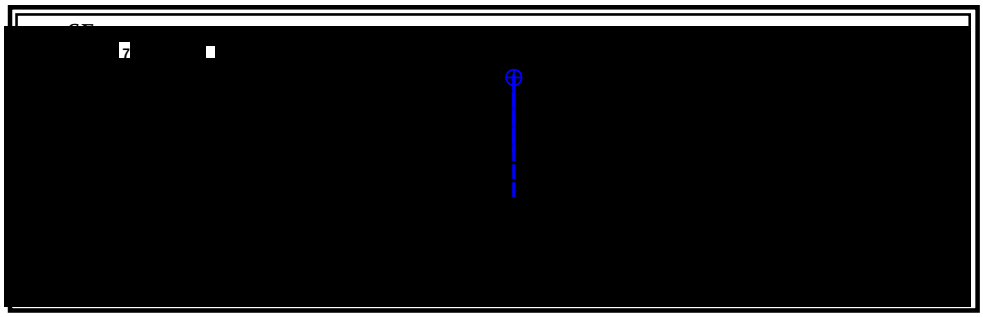

Fig. (16): Inverted resistivity model of the Two-Dimension imaging profile at the second site.

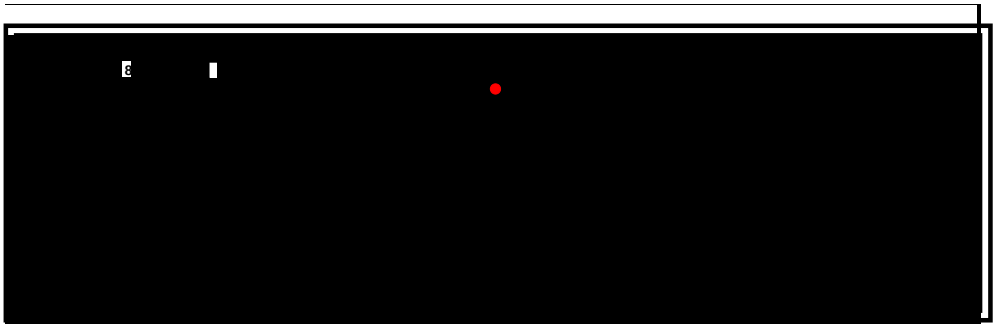

Fig. (17): Inverted resistivity model of the Two-Dimension imaging profile at the third site.

The last zone has resistivity values ranges from 500 to more than 1000 Ohm-m. These resistivity values correspond to crystalline basement. The depth to the top of this zone is about 130 m in the southeastern part and was not detected in the northwestern part due to the effect of structural fault (F2). This structural picture coincides and confirm well with that detected from the VES interpretation results.

The true resistivity plot of the 2-D imaging profile at site two (Fig. 16) indicates that, this model consists of two zones, according to the resistivity values along the profile. The upper zone is dry. It consists of two layers which are equivalent to the Quaternary alluvium. The upper layer has a wide resistivity range that varies from about 60 to more than 500 Ohm-m. This zone is equivalent to the dry gravel, boulders, sand and sandstone. The thickness of this layer reaches as much as 27 m. The second layer has resistivity values ranging from 1 to 8 Ohm-m which correspond to clay deposits. This layer extends to a depth of about 67 m. The second zone represents the water-bearing formation and its resistivity values increase with depth from about 15 Ohm-m to about 120 Ohm-m. Therefore, the clay content decreases with depth and inversely, sand and sandstone percentage increase. The bottom of this layer was not reached up to a depth of 160m. with the used current electrode separation. These results coincide well with the interpretation results at VES 7 (Geoelectrical cross-section A-A', Fig. 5) which represents a grabben between site 1(VES 6) and site 3 (VES 8). Therefore, the bottom of the second zone and the following third zone (crystalline basement) were not reached.

The true resistivity plot of the Two-D imaging profile at the third site at VES no. 8 (Fig. 17) revealed that, the section consists of three zones. The upper one represents the dry zone which consists of two geoelectric layers. The upper layer has resistivity values ranging from 26 to more than 500 Ohm-m which corresponds to gravel, boulder, clay, sand and sandstone. Its thickness reaches about 22 m. The second one has a resistivity varies from less than 1 to 8 Ohm-m. These resistivity values correspond to clay deposits.

The second zone represents the water-bearing formation and its resistivity values increase with depth from about 16 Ohm-m to about 150 Ohm-m. Therefore, the clay content decreases downward and inversely, sand and sandstone percentage increase in the same trend. This phenomenon coincides with the previous two sites. The last zone has resistivity values ranges from about 400 to more than 900 Ohm-m. which correspond to crystalline basement rocks. The depth to the top of this zone is about 125 m.

From the interpretation results of the Two-Dimensional imaging profiles at the three sites, the following could be concluded:

The geoelectrical succession detected from the Two-Dimensional imaging profiles at the three sites coincid well with that detected from the interpretation results of Vertical Electrical Soundings.

In relation to the structure picture, site two (location of VES 7) represents a graben, where the bottom of the second zone (water-bearing formation) which equivalents to the top of the third zone (crystalline basement) was not reached comparable with the other two sites. On the other hand, each of the profiles at site three (location of VES 8) and the southeastern part of site one (location of VES 6) represents uplifted sites comparable with that at the second site where the third zone which represents the crystalline basement was detected. The top of the third zone that equivalent to the crystalline basement and in the same time represents the bottom surface of the second zone (water-bearing formation) was not reached at the northwestern part of the profile at the first site. This confirmed well with the detected graben at the Northwestern part of VES 6 precisely at VES 3 (geoelectrical cross-section A-A', Fig. 5).

Therefore, if the three two-D imaging profiles collected in one figure this will give the structural picture delineated in the geoelectrical cross-section A-A' especially at VESes nos. 3, 6, 7 and 8. Accordingly, it can be concluded that the Two Dimension imaging profiles coincide and confirm well with the reliability of the detected structure fault elements from the constructed geoelectriacal cross-sections.

CONCLUSION

To achieve the objective of this study, geoelectrical techniques in the form of Vertical Electrical Soundings and Two-Dimensional Electrical imaging were used. The quantitative interpretation of the geoelectrical resistivity sounding data as well as the constructed geoelectrical cross-sections led to the detection of three main geoelectrical zones (A, B and C), which correspond to Quaternary deposits, Cambrian Araba sandstone, and Precambrian basement rocks respectively. According to the results of this geophysical study, the following could be summarized:

1- The water-bearing formations in the study area are represented by geoelectrical unit "B" (Cambrian Araba sandstone). This unit is differentiated into three connected geoelectrical layers (B1, B2 and B3) without confining. These layers are composed of sand, clay and sandstone with different ratios. The clay percentage of these layers decreases with depth. The thickness of these layers is variable due to structural effect.

2- As the resistivity values give indication about the relative quality of groundwater and the thickness of water-bearing layer is a function in the quantity of groundwater as well as drilling large depths means much costs. These three factors are weighted to construct groundwater priority map for the integrated three layers (B1, B2 &B3) in the investigated area. The priority map indicates that, the southeastern part (VES nos. 8 and 9 followed by 10) represents the most promising area for drilling well to exploit the groundwater. The following priority is represented at

the extreme south (VES 12) and at local site in the northwestern part (VES 3).

3- The depth and level to the basement surface is variable along the study area. The minimum depth value attaining 90 m. was recorded at the south. On the other hand, the maximum value was recorded at the northwestern part. Generally, the depth and level decreases southeastwards except anomalous high and low values were detected at some sites in the middle part of the studied wadi due to the structure effects.

4- The geological setting that affect the basement surface and in turn the overlying water-bearing Cambrian Araba sandstone especially, the last layer "B3" was deduced from both the constructed geoelectrical cross-sections and the generated level basement map. It is represented by a group of normal faults (F1, F2 …F7). These faults form consecutive alternation of grabbens and horsts basement surfaces along the NW-SE main channel of Wadi Morra. Therefore, these faults have a major effect on the thickness of the Cambrian Araba water-bearing aquifer. This in turn has a major role in the occurrence and potential of groundwater.

5- To support the structural picture which is delineated from the constructed geoelectrical cross-sections, three two-Dimension electrical imaging profiles have the same length are interpreted. The interpretation results of the 2-Dimension imaging profiles at three sites coincide and confirm well with the reliability of the detected structure fault elements from the constructed geoelectriacal cross-sections.

In conclusion although the geologic setting plays a major role in lithologic facies changes and the thickness of the water-bearing aquifer, the area of study has a good groundwater potential except one site has a fair potential.

REFERENCES

Abdel Mogheeth, S.M., Misak, R.F., Atwa, S.M., Abdel Baki, A.A., and Salluma, M.K., (1988): On the chemical properties of the groundwater in selected fractured granitoids in Sinai and Eastern Desert, Egypt. Desert Institute Bull., A.R.E., Vol. 38/1 pp. 19-40.

Aggour, T.A., (2000): Priorities of flood insurance, Gulf of Aqaba region, Southeast Sinai Egypt. Desert Institute Bull. Vol. 49/2.

Bentor, Y.K., (1985): The crustal evolution of the Arabo-Nubian massive with special reference to the Sinai Peninsula, Precambrian Research, Vol. 28, pp. 1-74..

De Groot-Hedlin, C. and Constable, S. (1990): "Occam's inversion to generate smooth, two-dimensional models from magnetotelluric data" Geophysics, 55, 1613-1624.

El Ghazawi, M.M., 1999): Reconsideration of the hydrogeologic setting in the delta of Wadi Watier, Southeast Sinai. Mans. Sci. Bull. (CNat. Sci. and Phy. Sci.) Vol. 26/1, p. 23-47.

El Kiki, M.F., Eweida, E.A. and El Refai, A.A., (1992): Hydrogeology of the Aqaba rift porderprovinc. Proc. 3rd Conf. Geol. Sinai Develop., Ismailia, p. 91-100.

El Shafei, M. K., Khawasik, S.M., and El-Ghawaby, M.A., (1992): Deformational styles in the tectonites of Wadi Saal, South Sinai. Proceed. Of the 3rd Conf. on Geology of Sinai Develop., Ismailia, Egypt, pp. 1-8.

El Shamy, I.Z., (1992): Towards the water management in Sinai Peninsula. Proc. 3rd Conf. Geol. Sinai Develop., Ismailia, p. 63-70.

Eyal, M., Eyal, Y., Bartov, Y., and Steinitz, G., (1981): The tectonic development of the western margin of the Gulf of Wlat (Aqaba) rift. Elsevier Sc. Publ. Comp.., Amesterdam, Netherland, Tectonophysics, Vol. 80, p. 39-66.

Geological Survey of Egypt (G.S.E), (1994): Geological map of Sinai, Scale 1:250,000. Geol. Surv. Egypt, Cairo, Egypt. Sheet no. 1.

Griffiths, D.H. and Barker, R.D. (1993): Two-dimensional resistivity imaging and modeling in areas of complex geology. Jour. of Applied Geoph., 29, Elsevier Science Publishers, B.V., Amsterdam, pp. 211-226.

Hammad, F.A. and Misak, R.F., (1985): Quantitative geomorphology and groundwater possibilities in the vicinities of Wadi Nassib, Abu Zenima, Sinai. Desert Inst. Bull. A.R.E., Vol. 35/2, p. 331-351.

Hasanein, A.M., (2007): Comparative study of the effective geomorphologic and geologic features on the water resources in Wadis Baba and Dahab, South Sinai, Egypt. Sed. of Egypt, Ain Shams Univ. Vol. 15, p. 35-52.

Hassan, A.A., (1967): A new Carboniferous occurrence in the Abu Durba, Sinai, Egypt. 6th Arab. Petrl. Congr., Baghdad, 2, 8pp.

Interpex Limited. (1996): RESIX- PLUS. Resistivity data interpretation software, v. 2.39., Golden, Colorado,USA.

Loizenbauer, J., Wallbrecher, E., Fritz, H., Neumayer, P., Khudeir, A.A., and Kloetzli, U., (2001): Structural geology, Single zircon ages and fluid inclusion studies of the Meatiq metamorphic core complex implication for Neoproterozoic tectonics in the Eastern Desert of Egypt. Precambrian research, Vol. 110, pp. 357-383.

Loke, M.H. and Barker, R.D. (1996a): Rapid least-squares inversion of apparent resistivity pseudo-sections by a quasi-Newton method. Geophysical prospecting, 44, pp. 131-152.

Loke, J., (1998) RES2DINV. V. 3.4, rapid 2-D resistivity inversion using the least-square method. ABEMinstrument AB, Bromma, Sweden.

Masoud, A.A. and Koike, K., (2011): Morphotectonics inferred from the analysis of topographic

Lineaments auto-detected from DEMs : Application and validation for the Sinai Peninsula, Egypt. Tectonophysics Jour. Vol. 510, pp. 291-308.

Saad, K.F., El Shamy, I.Z. and Sewedan, A.S., (1980): Quantitative analysis of the geomorphology and hydrology of Sinai Peninsula. Annals of the Geol. Surv. Egypt. Vol. 10, p. 819-836.

Said, R. (1962) The Geology of Egypt, Elsevier Publ. Co., Amsterdam, 377p.

Shabana, A.R., (1999): Geology of water resources in some catchment areas drainage in the Gulf of Aqaba, Sinai, Egypt. Ph.D Thesis, Geol. Dept. Fac. Sci. Ain Shams Univ. 257pp.

Shimron, A., (1984): Metamorphism and tectonics of a Pan African terrain in southeastern Sinai. A discussion. Precambrian Research, Vol. 24, pp. 173-188.

Stern, R.J., (1994): Arc assembly and continental collision in the Neoproterozoic Wast African Orogen Implications for the consolidation of Gondwana land. Ann. Rev. Earth Sci. Vol. 22, pp. 319- 351.

Telford, W.M., Geldart, L.P., Sheriff, R.E., (1990): Applied geophysics. Cambridge Univ. Press; 2nd Edition 752 p.

Van Der Velpen, B.P.A., (1988): RESIST. Version 1.0, a package for the processing of the resistivity sounding data: M. Sc. Research Project, ITC, Delft, the Netherlands.